Swine interferon-induced transmembrane protein, sIFITM3, inhibits foot-and-mouth disease virus infection *in vitro* and *in vivo*

Jinfang Xu [a,b], Ping Qian [a,b], Qunfeng Wu [a,b], Shasha Liu [a,b], Wenchun Fan [a,b], Keshan Zhang [c], Rong Wang [a,b], Huawei Zhang [a,b], Huanchun Chen [a,b], Xiangmin Li [a,b,∗]

[a] State Key Laboratory of Agriculture Microbiology, Huazhong Agricultural University, Wuhan 430070, China
[b] Division of Animal Infectious Diseases, College of Veterinary Medicine, Huazhong Agricultural University, Wuhan 430070, China
[c] Chinese Academy of Agricultural Sciences, Xujiaping 1, Lanzhou 730046, China

ARTICLE INFO

ABSTRACT

The interferon-induced transmembrane protein 3 (IFITM3) is a widely expressed potent antiviral effector of the host innate immune system. It restricts a diverse group of pathogenic, enveloped viruses, by interfering with endosomal fusion. In this report, the swine IFITM3 (sIFITM3) gene was cloned. It shares the functionally conserved CD225 domain and multiple critical amino acid residues (Y19, F74, F77, R86 and Y98) with its human ortholog, which are essential for antiviral activity. Ectopic expression of sIFITM3 significantly inhibited non-enveloped foot-and-mouth disease virus (FMDV) infection in BHK-21 cells. Furthermore, sIFITM3 blocked FMDV infection at early steps in the virus life cycle by disrupting viral attachment to the host cell surface. Importantly, inoculation of 2-day-old suckling mice with a plasmid expressing sIFITM3 conferred protection against lethal challenge with FMDV. These results suggest that sIFITM3 is a promising antiviral agent and that can safeguard the host from infection with FMDV.

1. Introduction

The innate immune system is the first line of defense against pathogenic invasion (Tarakhovsky and Kroemer, 2012). Type I/II interferons (IFNs) are critical for generating cell intrinsic antiviral activity and hindering pathogens infection by inducing expression of a large number of IFN-stimulated genes (ISGs) (Liu et al., 2012). The human IFN-induced transmembrane protein 3 (IFITM3) was recently identified as a new antiviral effector of the ISGs family. Overexpression of IFITM3 blocks infection of a wide range of highly pathogenic enveloped viruses, including influenza A virus (IAV), vesicular stomatitis virus (VSV), West Nile virus, dengue virus, and severe acute respiratory syndrome coronavirus, as well as one non-enveloped reovirus (Anafu et al., 2013; Brass et al., 2009; Huang et al., 2011; Weidner et al., 2010).

IFITM3 is a small ISG protein with an approximate molecular weight of 15 kDa, and it belongs to the cluster of differentiation 225 (CD225) domain family (John et al., 2013). Amino acid (aa) sequence analysis of IFITM3 and its other four human paralogs (IFITM1, IFITM2, IFITM5 and IFITM10) reveals that they have two intramembrane domains (IM1 and IM2) and a conserved intracellular loop (CIL), flanked by short variable N-terminal and C-terminal domains (John et al., 2013). The intramembrane domains and CIL constitute the CD225 domain that is shared by hundreds of CD225 domain family members (Punta et al., 2012). Brass et al. (2009) first demonstrated the antiviral activity of IFITM proteins using a functional RNAi genomic screen. IFITM3 expression accounted for 50–80% of IFNs' ability to block IAV infection and exhibited early viral infection restriction (Brass et al., 2009). IFITM3 potently restricts the viral entry by altering the properties of cellular endolysosomal membranes, thus creating an unfavorable milieu for viral fusion with membranes (Amini-Bavil-Olyaee et al., 2013; Feeley et al., 2011). IFITM3 further blocks cytosolic entry of viruses and the release of viral genomes, resulting in degradation of pathogens trapped within later endosomal or lysosomal compartments.

Foot-and-mouth disease virus (FMDV) is a non-enveloped virus with a positive single-stranded RNA genome of approximately 8.5 kb, enclosed within an icosahedral capsid formed from 60 copies of four structural proteins (VP1, VP2, VP3 and VP4) (Grubman and Baxt, 2004). FMDV has seven serotypes, A, O, C, Asia 1, SAT 1, SAT 2, and SAT 3, with little cross-protection (Bronsvoort et al., 2008; Cao et al., 2013; Rodriguez and Gay, 2011). These make it difficult to prevent and control FMDV by current vaccines (Golde et al., 2005). Studies have demonstrated that FMDV is sensitive

to the action of α/β-IFNs (Dias et al., 2012; Golde et al., 2008; Kim et al., 2012; Molinari et al., 2010). Inoculation of swine with adenovirus-delivered type I IFN confers 100% protection against FMDV-caused fever, vesicular lesions, and viremia and this protection can be maintained for 3–5 days (Chinsangaram et al., 2003). In addition, IFNs interact with cognate receptors on the cell surface and activate ISGs expression to safeguard the host through intracellular signaling cascades (Siegrist et al., 2011).

FMDV enters host cells *via* receptor recognition and clathrin-dependent endocytosis. Later, an acidic pH within the endosome is required to disassemble the capsid and translocate viral RNA into the cytoplasm (Johns et al., 2009). Ebola virus, IAV and VSV that exhibit similar entry patterns are inhibited by human IFITM3 (Bhattacharyya et al., 2010; Huang et al., 2011; Lakadamyali et al., 2004; Sun et al., 2005; Weidner et al., 2010). The aim of this study was to clone swine IFITM3 (sIFITM3) and examine if it could restrict FMDV infection. Our results demonstrate that sIFITM3 has a similarly functional CD225 domain and several critical conserved aa residues that correspond to its human ortholog. Ectopic expression of sIFITM3 inhibited infection of non-enveloped FMDV in baby hamster kidney (BHK-21) cells by disrupting viral attachment, and this differs from human IFITM3 restriction on enveloped viruses. Inoculation of suckling mice with a plasmid expressing sIFITM3 confers protection against lethal FMDV challenge. These data suggest that sIFITM3 is a novel and potent antiviral agent that could be used to enhance animal resistance to FMDV infection.

2. Materials and methods

2.1. Cell lines and viruses

BHK-21 and 293FT cells were grown in Dulbecco's modified Eagle's medium (DMEM; Invitrogen, USA) containing 10% fetal bovine serum, 100 U/ml penicillin, and 10 μg/ml streptomycin sulfate at 37 °C in a humidified 5% CO_2 incubator. Type O FMDV strains O/ES/2001, O/GD/2010, O/AH/2010 and type Asia 1 FMDV strain Asia 1/JS/2005 were amplified, and titrated by plaque assay and/or 50% tissue culture infective dose ($TCID_{50}$) assay in BHK-21 cells (Pengyan et al., 2008).

2.2. Cloning of sIFITM3 and plasmids construction

A BLAST search identified a swine expressed sequence tag (EST) sequence with high homology to the human IFITM3 sequence (GenBank: NM_080657.4). A reverse primer (sIFITM3-R: 5′-CTAGTA GCCTCTGTAATCCTTTATGAGC-3′) was designed using this EST sequence, and a forward degenerate primer (sIFITM3-F: 5′ -ACCATG AACTGCGCTTCCCAG-3′) was designed *via* multiple sequence alignment with human and predicted bovine IFITM3 (XM_850270.1). The cDNA of sIFITM3 was amplified by reverse transcriptase-polymerase chain reaction (RT-PCR) using total RNA extracted from a swine lymph node. The PCR product was cloned into the pMD18-T vector (Takara Bio Inc, Japan) for sequence verification.

The coding region of sIFITM3 was subcloned into the pLenti7.3/V5-GW/lacZ vector (Invitrogen) at *Bam*H I/*Xho* I sites to replace the lacZ gene, resulting in pLenti7.3-sIFITM3. It was also subcloned into the previously described pCA vector (Niwa et al., 1991), resulting in pCA-sIFITM3.

2.3. Generation of recombinant lentiviruses and establishment of stable cell lines

Briefly, 293FT cells were seeded at a density of 5×10^6 cells per 10 cm tissue culture plate and co-transfected with pLenti7.3-sIFITM3 or pLenti7.3-eGFP (expressing the emerald green

fluorescence protein, eGFP) and ViralPower™ Packaging Mixture (Invitrogen) using Lipofectamine 2000 (Invitrogen). Fresh medium was added 12 h later. The pseudotyped lentiviruses LV-sIFITM3 expressing sIFITM3 and LV-eGFP expressing eGFP were collected 48 h and 72 h post transfection and filtered through a 0.45 μm filter. BHK-21 cells were transduced by incubation with equal volumes of fresh DMEM and lentivirus containing medium in the presence of 4 μg/ml of polybrene. Twenty-four hours post transduction, cell clones were developed by limiting dilution of the cell populations expressing sIFITM3 or eGFP. The BHK-21 stable cell lines expressing sIFITM3 (BHK-sIFITM3) or expressing eGFP (BHK-eGFP) were identified by fluorescence microscopy analysis and Western blotting assay.

2.4. Viral attachment and viral entry assays

BHK-sIFITM3 or BHK-eGFP were seeded in six-well plates at a density of 5×10^5 cells per well and cultured for 12 h. Next, cells were ice-chilled and incubated with FMDV strain O/ES/2001 (henceforth referred to as O/ES/2001) at a multiplicity of infection (MOI) of 10 for 1 h on ice to allow viral attachment but impede viral entry. After three washing steps with ice-cold phosphate-buffered saline (PBS), O/ES/2001 binding to the host cell surface was measured by real-time quantitative RT-PCR and flow cytometric analysis. To assay viral entry into cells, viral inocula were removed after 1 h of binding on ice. Cells were intensively washed with ice-chilled PBS, and pre-warmed medium was added, followed by incubation for an additional 10 min at 37 °C incubator. This was followed by one washing step with cold PBS, treatment with 0.25% trypsin, and three more washing steps with cold PBS to remove any cell-associated virions that had not entered the cytoplasm. Real-time RT-PCR and plaque assay were used to determine the amount of virus that had entered cells.

2.5. Quantification of FMDV by real-time RT-PCR

BHK-sIFITM3 or BHK-eGFP cell lines were cultured for 12 h, followed by infection with O/ES/2001. Cells were harvested prior to being infected or at indicated time points post infection. Total cellular RNA or viral RNA were extracted with TRIzol reagent (Invitrogen), treated with DNase (Promega, USA) and reverse transcribed with ReverTra Ace® (Toyobo; Shanghai, China). Real-time PCR was performed with specific primers and/or probe targeted at the 2B gene of O/ES/2001 (2B: 5′-ACGAAACACGGACCCGACTT-3′/5′-CCTTGACCCCAGCGGCCAATTCCT-3′; probe: 5′-FAM-AACCGACT GGTGTCCGCGTTT-TAMRA-3′) in a LightCycler® 480 Real-Time PCR System (Roche; Indianapolis, IN, USA). Primers of β-actin (5′-GGTCATCACTATTGGCAACG-3′/5′-TCCATACCCAAGAAGGAAGG-3′) were used as an endogenous reference control. Thermal cycling conditions were 1 min at 95 °C, then 40 cycles of 15 s at 95 °C, 30 s at 60 °C and 45 s at 72 °C. Gene expression was analyzed as described previously (Li et al., 2009; Wu et al., 2009, 2011).

2.6. Titration of O/ES/2001 by $TCID_{50}$ and plaque assay

BHK-sIFITM3 and BHK-eGFP cell lines were seeded into six-well plates 24 h prior to infection with different doses of O/ES/2001. Cells and supernatants containing virus were collected at different time points and stored at −80 °C. To determine quantities of intracellular virus, cell suspensions were subjected to three freeze/thaw cycles to release virions. For $TCID_{50}$ assay, O/ES/2001 titer was determined by endpoint dilution as described previously (Pengyan et al., 2008). Briefly, 10-fold serial dilutions of FMDV samples were incubated in eight replicates in 96-well plates with 60–80% confluent BHK-21 cells. Two hours later, the supernatant was replaced with fresh culture medium. Plates were incubated

for an additional 24–48 h to determine cytopathic effect (CPE). The $TCID_{50}$ was calculated with Reed–Muench formula (Reed and Muench, 1938). For plaque assay, BHK-21 cells were seeded in six-well plates 24 h prior to infection with 10-fold serially diluted O/ES/2001 samples. A 2% methylcellulose overlay was added post 2 h incubation. Plaques were fixed with 10% formaldehyde and visualized with crystal violet staining 48 h post infection.

2.7. Flow cytometric analysis

Infected or non-infected BHK-sIFITM3 and BHK-eGFP cells were detached with trypsin, washed with PBS by centrifugation at 250 g for 5 min, and fixed with 4% paraformaldehyde. Cells were washed and suspended with solution containing an anti-VP1 monoclonal antibody (mAb) (1:100 dilution; prepared in our laboratory) for 1 h at room temperature, followed by three round of washing steps. After centrifugation, the cells were stained with goat anti-mouse Cy3-conjugated secondary antibody (Abcam, USA). Finally, cells were washed, resuspended in PBS and analyzed by flow cytometry FACSCalibur (BD BioSciences, USA). The percentage of eGFP- and Cy3-positive cells in each sample was analyzed with the CellQuest software (BD BioSciences).

2.8. Western blotting assay

The protein concentration of cell lysates was determined with bicinchoninic acid protein assay kit (Pierce, USA). Equal protein amounts were separated using 12% sodium dodecyl sulfate–polyacrylamide gel electrophoresis and transferred onto a nitrocellulose membrane. The membrane was blocked with 5% non-fat milk and incubated with primary rabbit anti-sIFITM3 polyclonal antibody (1:1000 dilution; prepared in our laboratory), probed with a secondary peroxidase-conjugated anti-rabbit antibody (Sigma, USA), followed by enhanced chemiluminescence staining (Thermo Fisher, USA). Expression of β-actin was detected with an anti-β-actin mAb (Sigma) as internal reference.

2.9. Inoculation of suckling mice and viral challenge

Groups of 2-day-old suckling mice (9–10 mice/group) were obtained from the Wuhan Institute of Biological Products of China National Biotec Cooperation (Wuhan, China). They were housed and handled according to the Hubei Provincial Animal Care and Use Committee Guidelines. The mice were inoculated subcutaneously with 25 μl (1 μg/μl) pCA-sIFITM3, pCA or 25 μl PBS as control. At 48 h post immunization, the mice were subcutaneously infected with 5 mouse lethal dose 50 (MLD_{50}) of O/ES/2001 at the immunization site. The mice were observed for clinical signs for 2 weeks.

2.10. Statistical analysis

All data were analyzed with one-way analysis of variance by the Origin 8 software (Origin Lab; Northampton, MA, USA). P values <0.05 were considered statistically significant. The survival curves were analyzed with the Kaplan–Meier method and compared with a log-rank test (χ^2 test) (Wu et al., 2013).

3. Results

3.1. Cloning and sequence analysis of sIFITM3

The sIFITM3 fragment was amplified by RT-PCR from the swine lymph node with primers sIFITM3-F and sIFITM3-R. The full-length cDNA of sIFITM3 is 438 base pairs (bp) and it encodes 145 aa residues (GenBank: HQ641403.1).

Multiple sequence alignments against IFITM3 sequences from other species show that sIFITM3 nucleotide sequence shares 82% identity with bovine IFITM3, 71% with human IFITM3, 65% with mouse IFITM3 and 37% with chicken IFITM3. Corresponding aa alignments exhibit 71%, 66%, 58% and 32% identity, respectively (Fig. 1A). Phylogenetic analysis indicates that sIFITM3 belongs to the group containing bovine IFITM3 (Fig. 1B).

To predict the functional characteristics of sIFITM3, the putative aa sequence was compared with human IFITM3. sIFITM3 protein sequence is 12 aa longer than its human ortholog, and heterogeneity is mainly displayed at the C-terminal (Fig. 1C). Comparison of the sIFITM3 and human IFITM3 functional domains shows that aa residue identity is 100% at the N-terminal domain (NTD), 91% at the IM1 domain, 86% at the CIL domain, 35% at the IM2 domain, and 72% at the CD225 domain overall, indicating that the functional domains are conserved between human and swine (Fig. 1C and D). In particular, sIFITM3 aa residues Y19, F74, F77, R86, and Y98 (corresponding to human IFITM3 aa residues Y20, F75, F78, R87, and Y99) are completely retained (Fig. 1C; highlighted with asterisk). These domains and residues are required for antiviral activity and cellular distribution of human IFITM3 (Jia et al., 2012; John et al., 2013). Importantly, these data suggested that sIFITM3 might possess the potential antiviral activity as its human ortholog.

3.2. Generation of BHK-21 stable cell lines

To investigate the antiviral activity of sIFITM3, we constructed the pseudotyped lentiviruses LV-sIFITM3 and LV-eGFP (Fig. 2A). BHK-21 cells were transduced with these lentiviruses to generate the stable cell lines BHK-sIFITM3 and BHK-eGFP. Western blotting assay confirmed that sIFITM3 was efficiently expressed in BHK-sIFITM3 cells (Fig. 2B). In addition, flow cytometric analysis showed that almost 100% of the cells were positive for sIFITM3 or eGFP expression (data not shown). These data demonstrated that these two cell lines could be used for the following antiviral study.

3.3. Expression of sIFITM3 robustly restricts FMDV infection

FMDV has several serotypes that do not confer cross-protection against each other. As such, we firstly evaluated the antiviral activity of sIFITM3 against different serotypes FMDV. Low MOI (MOI = 0.01) were used, as FMDV exhibits high replication ability and pathogenesis in BHK-21 cells. Two days post infection of the cell lines with viruses, plaque assay showed that BHK-sIFITM3 was less susceptible to infection by type O FMDV strains O/ES/2001, O/GD/2010, and O/AH/2010 than the control BHK-eGFP, and reduced plaque formation numbers by over 11- to 24-fold (Fig. 2C). In addition, post infection with type Asia 1 FMDV Asia 1/JS/2005, the plaque formation number was reduced to over 13-fold in BHK-sIFITM3 cells (Fig. 2C).

Next, FMDV viral RNA was quantified using real-time RT-PCR. sIFITM3 restricted the replication level of serotype O FMDV O/ES/2001, O/GD/2010 and O/AH/2010 about 5-fold, 6.5-fold and 7-fold lower, respectively, when compared with BHK-eGFP cells ($P < 0.01$) (Fig. 2D). Furthermore, replication of FMDV serotype Asia 1 (Asia 1/JS/2005) was inhibited approximately 9-fold in BHK-sIFITM3 cells when compared with BHK-eGFP cells ($P < 0.01$).

3.4. sIFITM3 inhibits O/ES/2001 infection by disrupting an early phase

To characterize the dynamic curve of viral infection inhibited by sIFITM3, the appearance of CPE and viral titers were monitored in
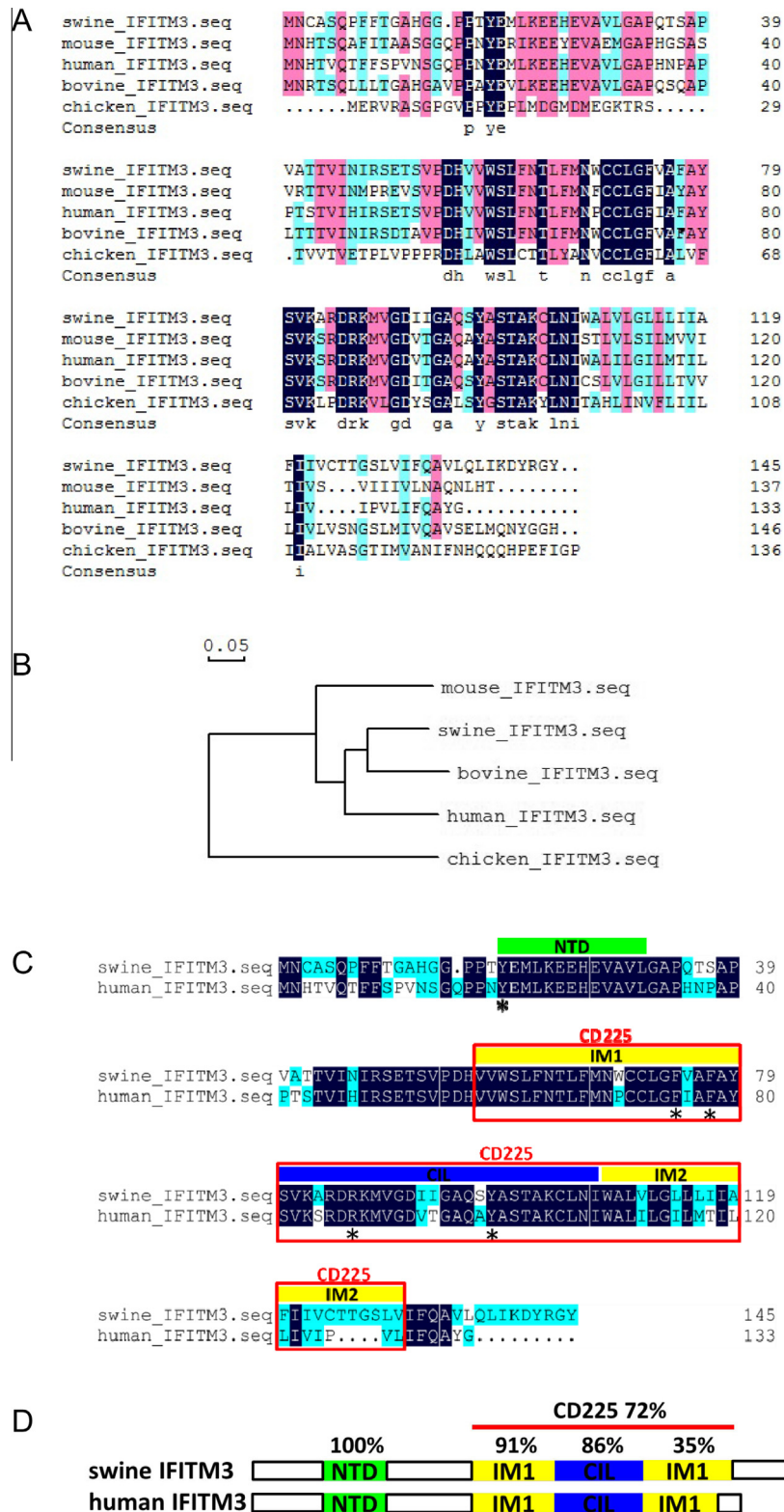
Fig. 1. Alignment, phylogenetic tree and architecture of sIFITM3. (A) Aa sequence alignment of swine, human, mouse, bovine, and chicken IFITM3. The numbers indicate the aa position. Identical aa residues (black) and similar aa residues (red is identity from 75% to less than 100% and blue is identity from 50% to less than 75%) are marked. (B) Phylogenetic tree for five identified or predicted IFITM3. Sequences are derived from GenBank accession numbers HQ641403.1 (swine), NM_021034.2 (human), NM_025378.2 (mouse), NM_181867.1 (bovine), and KC876032.1 (chicken). The uprooted tree was built using the neighbor-joining method and the scale bar is 0.05. (C) Analysis of functional domains of swine and human IFITM3. A schematic diagram of the N-terminal domain (NTD, green) and the CD225 domain (red box) with predicted intramembrane domain 1 (IM1), conserved intracellular loop (CIL), and intramembrane domain 2 (IM2) shown in yellow and blue. Critical and conserved residues are indicated with an asterisk. (D) Functional domain alignment of swine and human IFITM3. NTD, IM1, CIL, IM2 are shown in green, yellow, blue and CD225 with red line. (For interpretation of the references to color in this figure legend, the reader is referred to the web version of this article.)
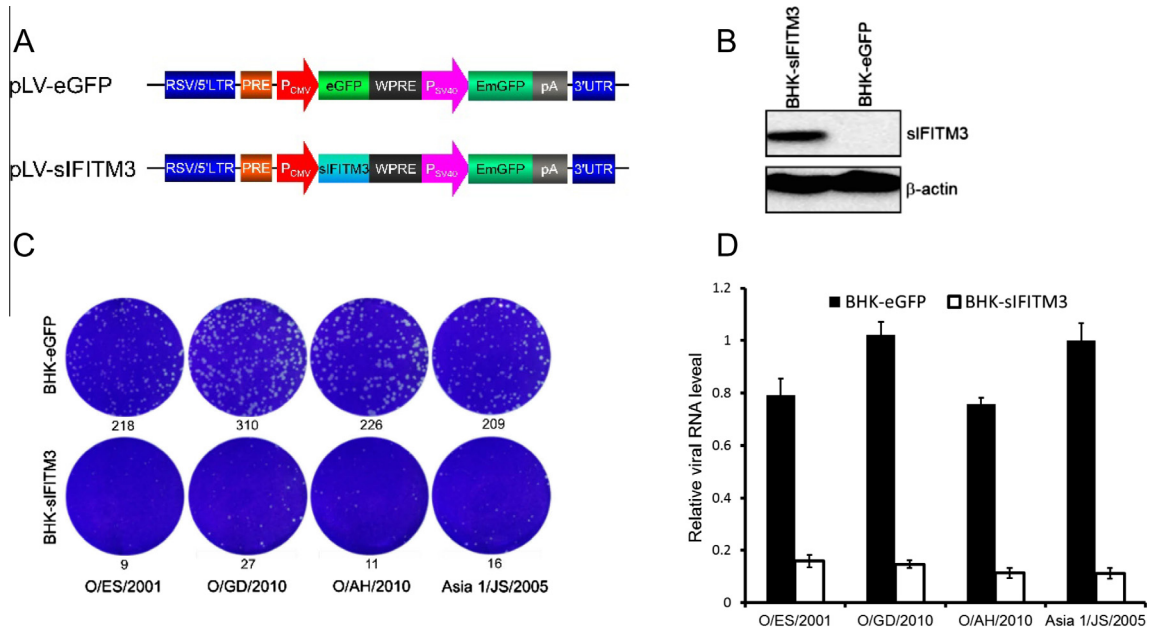
Fig. 2. sIFITM3 inhibits FMDV replication in BHK-21 cells. (A) Schematic diagrams of pLenti-eGFP and -sIFITM3 used to establish stable cell lines BHK-eGFP and BHK-sIFITM3. (B) sIFITM3 expression in BHK-sIFITM3 cells. (C) Plaque formation ability of FMDV strains in BHK-eGFP and BHK-sIFITM3 cells. The plaque numbers are presented underneath of the plates. (D) Viral RNA of FMDV strains as quantified by real-time PCR.

cells infected with O/ES/2001. O/ES/2001 caused obvious CPE in BHK-eGFP cells as early as 12 h post infection, and all cells were dead at 24 h post infection (Fig. 3A). In contrast, only slight CPE was observed in the BHK-sIFITM3 cells up until 24 h post infection.

Similarly, O/ES/2001 titers in cell supernatants collected at different time points post-infection were lower in BHK-sIFITM3 cells than in BHK-eGFP cells ($P < 0.01$) (Fig. 3B). As early as 6 h post infection, expression of sIFITM3 substantially inhibited O/ES/2001 production at least 100-fold, and cells maintained antiviral status as long as 36 h post-infection ($P < 0.01$) (Fig. 3A and B).

3.5. sIFITM3 restricts O/ES/2001 viral attachment

To determine the infection step specifically disrupted by sIFITM3, we first examined whether O/ES/2001 attachment and entry could be blocked by ectopic expression of sIFITM3 in BHK cells, with regard to the successive steps of virus infection. As

shown in Fig. 4A, sIFITM3 expression substantially blocked virus binding to cell surface, as viral RNA copies extracted from BHK-sIFITM3 cells were significantly fewer than those extracted from BHK-eGFP cells. To analyze viral entry, cells were incubated an additional 10 min at 37 °C, and real-time PCR was performed on intracellular viral RNA. The intracellular viral load was 9-fold lower in BHK-sIFITM3 cells than in BHK-eGFP cells ($P < 0.01$) (Fig. 4A). Moreover, plaque assay demonstrated that viral entry into BHK-sIFITM3 cells was significantly lower than that in BHK-eGFP cells ($P < 0.01$) (Fig. 4B).

To further confirm that sIFITM3 inhibits O/ES/2001 attachment to cell surface, the immunofluorescence and flow cytometric assays were performed to probe the virions binding on cell surface with mAb against O/ES/2001 VP1. Fluorescence intensity by microscope observation indicated that fewer virus particles were attached to cells expressing sIFITM3 when compared with control cells (data no shown). Moreover, flow cytometric analysis showed
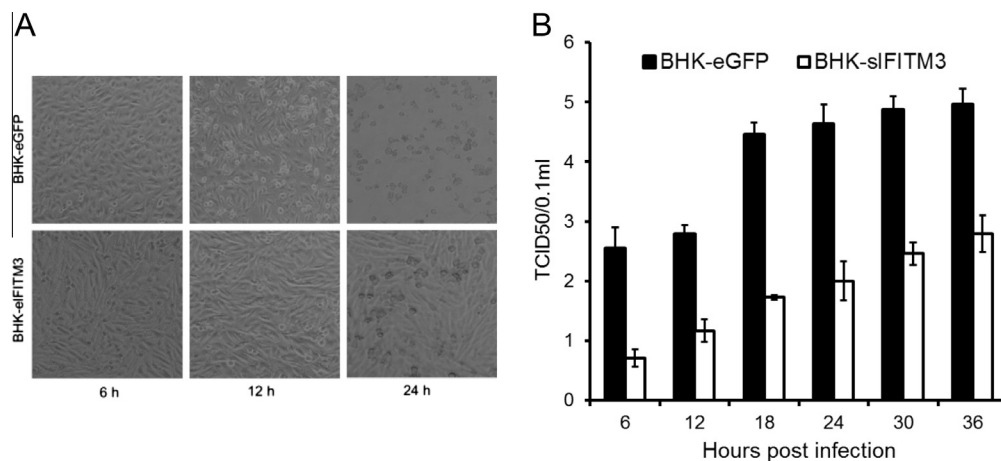

Fig. 3. sIFITM3 restricts FMDV infection by disrupting an early phase. (A) BHK-eGFP or BHK-sIFITM3 cells were infected with O/ES/2001 (MOI = 0.01). CPE was assessed at different time points post-infection. (B) Supernatants were harvested at different time points, and viral yield was measured by $TCID_{50}$. Error bars indicate standard deviations of mean values ($n = 3$).
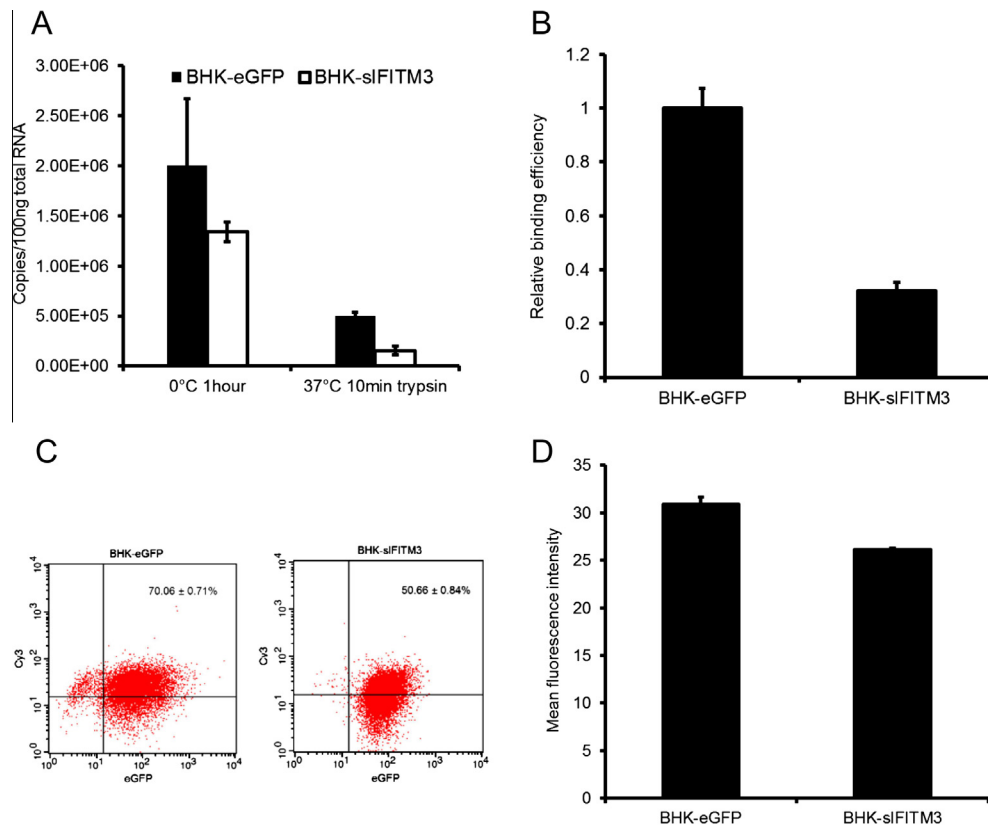
Fig. 4. sIFITM3 blocks FMDV infection at viral attachment step. (A) BHK-eGFP and BHK-sIFITM3 cells were infected with FMDV (MOI = 10). Intracellular viral RNA was extracted and quantified by real-time RT-PCR. Results indicate viral genome copies per 100 ng of total RNA. (B) FMDV particles that entered the cell cytoplasm as measured by plaque assay. (C and D) Flow cytometric analysis of viral attachment to cell surface. FMDV-binding cells were stained with anti-VP1 mAb and Cy3-conjugated secondary antibodies. (C) Percentage of virus-positive cells and (D) mean fluorescence intensity per positive cell.

that over 70% of BHK-eGFP cells exhibited an anti-VP1 mAb-positive signal, compared with less than 50% of BHK-sIFITM3 cells ($P < 0.01$) (Fig. 4C). Mean fluorescence intensity analysis showed that each BHK-eGFP cell captured more viral particles than BHK-sIFITM3 cell ($P < 0.01$) (Fig. 4D).

3.6. sIFITM3 protected suckling mice from O/ES/2001 challenge

Encouraged with the substantial antiviral effect of the sIFITM3 *in vitro*, we investigated the antiviral activity of sIFITM3 in suckling mice challenged with O/ES/2001. Two-day-old suckling mice were inoculated subcutaneously with 25 μg pCA-sIFITM3, pCA, or 25 μl PBS, then challenged with 5 MLD_{50} O/ES/2001 at the inoculation site 2 days later (Fig. 5A). All PBS-treated mice died within 5 days, and 88.8% of the pCA-treated mice died within 7 days post viral challenge (Fig. 5B). Six of the 10 mice inoculated with pCA-sIFITM3 survived the viral challenge, and this difference was statistically significant from the PBS and pCA control groups ($P < 0.01$). These data indicated that sIFITM3 conferred protection against lethal O/ES/2001 challenge in the suckling mice. One out of the nine mice in pCA group survived. It is possibly due to the non-specific innate immune response induced by plasmid DNA *in vivo*.

4. Discussion

IFNs are part of the first line of defense against pathogen invasion and they confer antiviral activity *via* several diverse mechanisms. Antiviral IFN signal amplification is primarily effected by ISG, and many ISG suppress virus infection at multiple steps in the virus life cycle (Sadler and Williams, 2008). IFITM3 is a transmembrane protein that is mainly stimulated by type I IFN. It has been implicated in a broad range of cellular processes including adhesion, apoptosis, immune cell signaling, oncogenesis cell adhesion, heart development, germ cell homing, and repulsion (Siegrist et al., 2011). IFITM3 is also responsible for IFN-induced cell growth inhibition by transduction of antiproliferative signals (Brem et al., 2003). However, our data show that expression of sIFITM3 in BHK-21 cells does not interfere with cell growth in comparison with the BHK-eGFP, as previous studies (data not shown) (Brass et al., 2009; Weidner et al., 2010). More importantly, IFITM3 is a potent antiviral effector against a number of viruses infection (Anafu et al., 2013; Brass et al., 2009; Jiang et al., 2010).

To date, the characteristics and antiviral activity of IFITM3 have been mainly investigated in human species and human-associated pathogens. Despite the moderate degree of inter-species similarity (71%) to the human ortholog, sIFITM3 shares the similar molecular structure with human IFITM3 and retains the highly conserved (100% identity) NTD with aa from 19 to 31. The conserved distal NTD is essential for complete antiviral activity of IFITM3, especially the critical tyrosine Y20 (Y19 in sIFITM3), whose dephosphorylation would result in mislocalization of IFITM3 from endosomes and lysosomes to the cell periphery and loss of the restriction of virus infection (Jia et al., 2012; John et al., 2013). sIFITM3 shares the 91% identity to IM1 and 86% identify to CIL of the main functional CD225 domain of human IFITM3 and still keeps all the conserved residues F74, F77, R86 and Y98, which are indispensable for viral inhibition, intermolecular interaction, protein trafficking and phosphorylation (John et al., 2013).

In this study, it has been observed that sIFITM3 acts at early steps in the FMDV life cycle, and these findings are consistent with
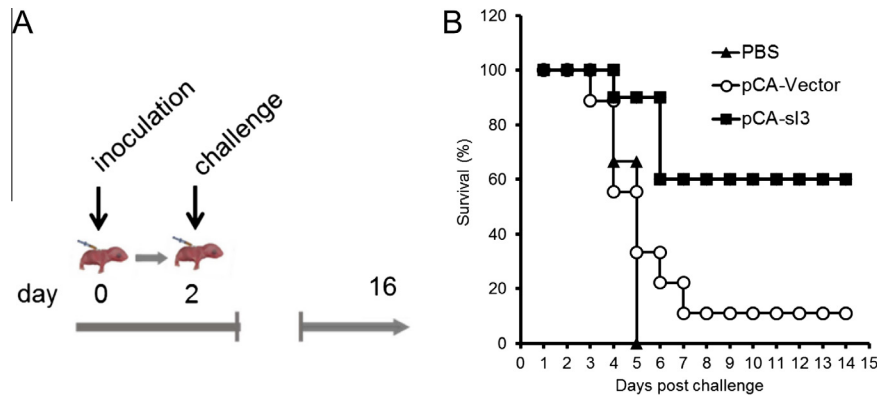
Fig. 5. sIFITM3 protects suckling mice from lethal FMDV challenge. (A) Schematic illustration of experimental procedure. Suckling mice were inoculated with 25 μg pCA-sIFITM3, pCA vector, or 25 μl PBS. Forty-eight hours later, mice were challenged with 5 MLD$_{50}$ FMDV O/ES/2001. (B) Survival curves for the immunized groups 14 days after viral challenge. $P < 0.01$; pCA-sIFITM3 versus pCA after viral challenge.

IFITM proteins to inhibit the early replication of IAV and flaviviruses (Brass et al., 2009). Surprisingly, we found that sIFITM3 disrupts FMDV attachment to the cell surface. This result differs from previous studies, in which human IFITM3 interferes with fusion of intraluminal virion-containing vesicles and endosomal membranes, thereby blocking genome release from IAV and VSV into the cytoplasm (Amini-Bavil-Olyaee et al., 2013; Feeley et al., 2011).

One recent study suggests that IFITM3 exerts antiviral effect by eliciting a marked accumulation of cholesterol within endosomes, ultimately impairing the function of endosome membrane-virus fusion (Amini-Bavil-Olyaee et al., 2013). In addition, integrins recycling on endosomes membrane serve as main receptors recognizing FMDV particles (Johns et al., 2009). Siljamaki et al. reported that cholesterol stability plays a vital role in integrin α2 uptake and in the formation of integrin-specific multi-vesicular bodies during virus infection (Siljamaki et al., 2013). Cholesterol aggregation can halt integrin α2 uptake and prevent internalization. It has also been reported that IFITM1, the paralog of IFITM3, interacts with hepatitis C virus receptors CD81 and occludin to disrupt the process of viral entry (Wilkins et al., 2013). In future studies, it will be interesting to explore the relationship between the biological features, steady state of FMDV receptors and sIFITM3 expression.

It has further been demonstrated that IFITM3 alters endosomal structure and its acidic milieu (Amini-Bavil-Olyaee et al., 2013; Anafu et al., 2013; Feeley et al., 2011). Therefore, we postulate that virus attachment is not the only step that is targeted by sIFITM3 during FMDV infection. We cannot exclude the possibility that sIFITM3 also alter endosomes in BHK-21 cells in order to prevent the disassembly of the viral capsids and viral RNA release. We suppose that the 3- to 4-fold decrease in viral attachment associated with sIFITM3 expression cannot fully account for over 100-fold decrease in viral production.

Control of animal infectious pathogens is a key component for the development of livestock farming. FMDV is a highly contagious disease among cloven-hoofed animals that can have a devastating economic impact on the international trade of animals and animal products (Carpenter et al., 2011; Yang et al., 1999). Our data indicate that sIFITM3 is a potent swine-originated factor defense against FMDV infection in BHK-21 cells and suckling mice. Therefore, we propose that this novel antiviral factor sIFITM3 could potentially be employed to improve animal resistance to FMDV infection.

Conflict of interests

All authors declare no competing interests.

References

Amini-Bavil-Olyaee, S., Choi, Y.J., Lee, J.H., Shi, M., Huang, I.C., Farzan, M., Jung, J.U., 2013. The antiviral effector IFITM3 disrupts intracellular cholesterol homeostasis to block viral entry. Cell Host Microbe 13, 452–464.

Anafu, A.A., Bowen, C.H., Chin, C.R., Brass, A.L., Holm, G.H., 2013. Interferon-inducible transmembrane protein 3 (IFITM3) restricts reovirus cell entry. J. Biol. Chem. 288, 17261–17271.

Bhattacharyya, S., Warfield, K.L., Ruthel, G., Bavari, S., Aman, M.J., Hope, T.J., 2010. Ebola virus uses clathrin-mediated endocytosis as an entry pathway. Virology 401, 18–28.

Brass, A.L., Huang, I.C., Benita, Y., John, S.P., Krishnan, M.N., Feeley, E.M., Ryan, B.J., Weyer, J.L., van der Weyden, L., Fikrig, E., Adams, D.J., Xavier, R.J., Farzan, M., Elledge, S.J., 2009. The IFITM proteins mediate cellular resistance to influenza A H1N1 virus, West Nile virus, and dengue virus. Cell 139, 1243–1254.

Brem, R., Oraszlan-Szovik, K., Foser, S., Bohrmann, B., Certa, U., 2003. Inhibition of proliferation by 1–8U in interferon-alpha-responsive and non-responsive cell lines. Cell. Mol. Life Sci. 60, 1235–1248.

Bronsvoort, B.M., Parida, S., Handel, I., McFarland, S., Fleming, L., Hamblin, P., Kock, R., 2008. Serological survey for foot-and-mouth disease virus in wildlife in eastern Africa and estimation of test parameters of a nonstructural protein enzyme-linked immunosorbent assay for buffalo. Clin. Vaccine Immunol. 15, 1003–1011.

Cao, Y., Lu, Z., Li, Y., Sun, P., Li, D., Li, P., Bai, X., Fu, Y., Bao, H., Zhou, C., Xie, B., Chen, Y., Liu, Z., 2013. Poly(I:C) combined with multi-epitope protein vaccine completely protects against virulent foot-and-mouth disease virus challenge in pigs. Antiviral Res. 97, 145–153.

Carpenter, T.E., O'Brien, J.M., Hagerman, A.D., McCarl, B.A., 2011. Epidemic and economic impacts of delayed detection of foot-and-mouth disease: a case study of a simulated outbreak in California. J. Vet. Diagn. Invest. 23, 26–33.

Chinsangaram, J., Moraes, M.P., Koster, M., Grubman, M.J., 2003. Novel viral disease control strategy: adenovirus expressing alpha interferon rapidly protects swine from foot-and-mouth disease. J. Virol. 77, 1621–1625.

Dias, C.C., Moraes, M.P., Weiss, M., Diaz-San Segundo, F., Perez-Martin, E., Salazar, A.M., De los Santos, T., Grubman, M.J., 2012. Novel antiviral therapeutics to control foot-and-mouth disease. J. Interferon Cytokine Res. 32, 462–473.

Feeley, E.M., Sims, J.S., John, S.P., Chin, C.R., Pertel, T., Chen, L.M., Gaiha, G.D., Ryan, B.J., Donis, R.O., Elledge, S.J., Brass, A.L., 2011. IFITM3 inhibits influenza A virus infection by preventing cytosolic entry. PLoS Pathog. 7, e1002337.

Golde, W.T., Nfon, C.K., Toka, F.N., 2008. Immune evasion during foot-and-mouth disease virus infection of swine. Immunol. Rev. 225, 85–95.

Golde, W.T., Pacheco, J.M., Duque, H., Doel, T., Penfold, B., Ferman, G.S., Gregg, D.R., Rodriguez, L.L., 2005. Vaccination against foot-and-mouth disease virus confers complete clinical protection in 7 days and partial protection in 4 days: use in emergency outbreak response. Vaccine 23, 5775–5782.

Grubman, M.J., Baxt, B., 2004. Foot-and-mouth disease. Clin. Microbiol. Rev. 17, 465–493.

Huang, I.C., Bailey, C.C., Weyer, J.L., Radoshitzky, S.R., Becker, M.M., Chiang, J.J., Brass, A.L., Ahmed, A.A., Chi, X., Dong, L., Longobardi, L.E., Boltz, D., Kuhn, J.H., Elledge, S.J., Bavari, S., Denison, M.R., Choe, H., Farzan, M., 2011. Distinct patterns of

IFITM-mediated restriction of filoviruses, SARS coronavirus, and influenza A virus. PLoS Pathog. 7, e1001258.

Jia, R., Pan, Q., Ding, S., Rong, L., Liu, S.L., Geng, Y., Qiao, W., Liang, C., 2012. The N-terminal region of IFITM3 modulates its antiviral activity by regulating IFITM3 cellular localization. J. Virol. 86, 13697–13707.

Jiang, D., Weidner, J.M., Qing, M., Pan, X.B., Guo, H., Xu, C., Zhang, X., Birk, A., Chang, J., Shi, P.Y., Block, T.M., Guo, J.T., 2010. Identification of five interferon-induced cellular proteins that inhibit west nile virus and dengue virus infections. J. Virol. 84, 8332–8341.

John, S.P., Chin, C.R., Perreira, J.M., Feeley, E.M., Aker, A.M., Savidis, G., Smith, S.E., Elia, A.E., Everitt, A.R., Vora, M., Pertel, T., Elledge, S.J., Kellam, P., Brass, A.L., 2013. The CD225 domain of IFITM3 is required for both IFITM protein association and inhibition of influenza A virus and dengue virus replication. J. Virol. 87, 7837–7852.

Johns, H.L., Berryman, S., Monaghan, P., Belsham, G.J., Jackson, T., 2009. A dominant-negative mutant of rab5 inhibits infection of cells by foot-and-mouth disease virus: implications for virus entry. J. Virol. 83, 6247–6256.

Kim, S.M., Park, J.H., Lee, K.N., Kim, S.K., Ko, Y.J., Lee, H.S., Cho, I.S., 2012. Enhanced inhibition of foot-and-mouth disease virus by combinations of porcine interferon-alpha and antiviral agents. Antiviral Res. 96, 213–220.

Lakadamyali, M., Rust, M.J., Zhuang, X., 2004. Endocytosis of influenza viruses. Microbes Infect. 6, 929–936.

Li, Y., Huang, X., Xia, B., Zheng, C., 2009. Development and validation of a duplex quantitative real-time RT-PCR assay for simultaneous detection and quantitation of foot-and-mouth disease viral positive-stranded RNAs and negative-stranded RNAs. J. Virol. Methods 161, 161–167.

Liu, S.Y., Sanchez, D.J., Aliyari, R., Lu, S., Cheng, G., 2012. Systematic identification of type I and type II interferon-induced antiviral factors. Proc. Natl. Acad. Sci. U.S.A. 109, 4239–4244.

Molinari, P., Garcia-Nunez, S., Gravisaco, M.J., Carrillo, E., Berinstein, A., Taboga, O., 2010. Baculovirus treatment fully protects mice against a lethal challenge of FMDV. Antiviral Res. 87, 276–279.

Niwa, H., Yamamura, K., Miyazaki, J., 1991. Efficient selection for high-expression transfectants with a novel eukaryotic vector. Gene 108, 193–199.

Pengyan, W., Yan, R., Zhiru, G., Chuangfu, C., 2008. Inhibition of foot-and-mouth disease virus replication in vitro and in vivo by small interfering RNA. Virol. J. 5, 86.

Punta, M., Coggill, P.C., Eberhardt, R.Y., Mistry, J., Tate, J., Boursnell, C., Pang, N., Forslund, K., Ceric, G., Clements, J., Heger, A., Holm, L., Sonnhammer, E.L., Eddy, S.R., Bateman, A., Finn, R.D., . The Pfam protein families database. Nucleic Acids Res. 40, D290–D301.

Reed, L., Muench, H., 1938. A simple method of estimating fifty per cent endpoints. Am. J. Hyg. 27, 493–497.

Rodriguez, L.L., Gay, C.G., 2011. Development of vaccines toward the global control and eradication of foot-and-mouth disease. Expert Rev. Vaccines 10, 377–387.

Sadler, A.J., Williams, B.R., 2008. Interferon-inducible antiviral effectors. Nat. Rev. Immunol. 8, 559–568.

Siegrist, F., Ebeling, M., Certa, U., 2011. The small interferon-induced transmembrane genes and proteins. J. Interferon Cytokine Res. 31, 183–197.

Siljamaki, E., Rintanen, N., Kirsi, M., Upla, P., Wang, W., Karjalainen, M., Ikonen, E., Marjomaki, V., 2013. Cholesterol dependence of collagen and echovirus 1 trafficking along the novel alpha2beta1 integrin internalization pathway. PLoS One 8, e55465.

Sun, X., Yau, V.K., Briggs, B.J., Whittaker, G.R., 2005. Role of clathrin-mediated endocytosis during vesicular stomatitis virus entry into host cells. Virology 338, 53–60.

Tarakhovsky, A.S., Kroemer, G., 2012. Innate immunity. Curr. Opin. Immunol. 24, 1–2.

Weidner, J.M., Jiang, D., Pan, X.B., Chang, J., Block, T.M., Guo, J.T., 2010. Interferon-induced cell membrane proteins, IFITM3 and tetherin, inhibit vesicular stomatitis virus infection via distinct mechanisms. J. Virol. 84, 12646–12657.

Wilkins, C., Woodward, J., Lau, D.T., Barnes, A., Joyce, M., McFarlane, N., McKeating, J.A., Tyrrell, D.L., Gale Jr., M., 2013. IFITM1 is a tight junction protein that inhibits hepatitis C virus entry. Hepatology 57, 461–469.

Wu, Q., Fang, L., Wu, X., Li, B., Luo, R., Yu, Z., Jin, M., Chen, H., Xiao, S., 2009. A pseudotype baculovirus-mediated vaccine confers protective immunity against lethal challenge with H5N1 avian influenza virus in mice and chickens. Mol. Immunol. 46, 2210–2217.

Wu, Q., Xiao, S., Fan, H., Li, Y., Xu, J., Li, Z., Lu, W., Su, X., Zou, W., Jin, M., Chen, H., Fang, L., 2011. Protective immunity elicited by a pseudotyped baculovirus-mediated bivalent H5N1 influenza vaccine. Antiviral Res..

Wu, Q., Xu, F., Fang, L., Xu, J., Li, B., Jiang, Y., Chen, H., Xiao, S., 2013. Enhanced immunogenicity induced by an alphavirus replicon-based pseudotyped baculovirus vaccine against porcine reproductive and respiratory syndrome virus. J. Virol. Methods 187, 251–258.

Yang, P.C., Chu, R.M., Chung, W.B., Sung, H.T., 1999. Epidemiological characteristics and financial costs of the 1997 foot-and-mouth disease epidemic in Taiwan. Vet. Rec. 145, 731–734.